DOI: 10.1002/ejic.200800054

A Phenanthroline Heteroleptic Ruthenium Complex and Its Application to Dye-Sensitised Solar Cells

Anna Reynal,[a] Amparo Forneli,[a] Eugenia Martinez-Ferrero,[a] Antonio Sanchez-Diaz,[a] Anton Vidal-Ferran,[a,b] and Emilio Palomares*[a,b]

Keywords: Dyes / Solar cells / Ruthenium / Heteroleptic complexes / Charge recombination / Electron transfer

We report here the synthesis and characterization of a new heteroleptic ruthenium(II) complex and its applications as efficient light-harvesting sensitizer in functional dye-sensitized solar cells. The relation between the interfacial charge-transfer processes that govern the device performance and the cell efficiency under illumination are also discussed.

Introduction

Bis(bipyridine)ruthenium complexes have been widely studied as efficient light-harvesting molecules when adsorbed onto the surface of mesoporous semiconductor thin films, which are used as working electrodes on dye-sensitised solar cells (DSSC).[1] Despite the low molecular extinction coefficient and the lack of absorbance in the near infrared region of the solar spectrum when compared to, for example, phthalocyanines, they have the best light-to-energy conversion efficiencies to date. During the last 10 years the molecule known as **N719** [chemical name: bis(tetrabutylammonium) *cis*-bis(isothiocyanato)bis(2,2′-bipyridyl-4,4′-dicarboxylato)ruthenium(II)] has been the paradigm of a molecular dye because of its high solar-to-electricity efficiency achieved when used as sensitizer in DSSC.[2] Hence, an interesting challenge for many researchers has been the design and synthesis of new ruthenium(II) complexes with enhanced properties such as slow back-electron transfer from the photo-injected electrons at the mesoporous semiconductor either with the oxidized dye or the electrolyte[3] as well as the dye long-term stability under device operation.[4] To this end, a successful strategy has been the design and synthesis of ruthenium(II) heteroleptic compounds where one of the 4,4′-dicarboxy-2,2′-bipyridines has been replaced by a more appropriate ligand. As an example Nazeruddin et al.[5] showed that the presence of a bipyridine on the ruthenium(II) complex bearing long alkyl chains {common name: **Z907**, chemical name: *cis*-[bis(2,2′-bipyridyl-4,4′-dicarboxylic acid)(4,4′-dinonyl-2,2′-bipyridyl)bis(isothiocyanato)ruthenium(II)]} improves not only the device stability but also its performance under illumination at full sun light (100 mW/cm^2 1.5 AM G). The same strategy has been applied by Zakeeruddin and co-workers with **K77** dye [*cis*-{4,4′-bis[2-(4-*tert*-butoxyphenyl)ethenyl]-2,2′-bipyridyl}bis(2,2′-bipyridyl-4,4′-dicarboxylic acid)bis(isothiocyanato)ruthenium(II)] which, in combination with a non-volatile electrolyte, exhibits a unique performance by combining high efficiency and stability.[6] Thelakkat and co-workers[7] have also reported the use of tris(phenylamine)-substituted bipyridines in Ru^{II} complexes as efficient sensitizers for solid-state DSSC when using an organic hole conductor as a solid electrolyte.

In this communication we would like to report the synthesis and characterization of a new heteroleptic ruthenium(II) complex with one of the bipyridine ligands replaced by a more conjugated ligand such as the 5,6-dimethyl-1,10-phenanthroline. Scheme 1 illustrates the molecular structure of the ruthenium(II) heteroleptic complex. Moreover, we have also carried out a study of the interfacial charge-transfer kinetics of the molecule when anchored onto the surface of nanocrystalline TiO_2 semiconductor particles.

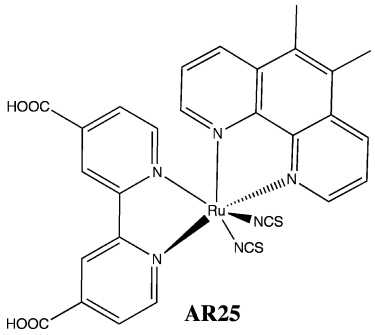

AR25

Scheme 1. Molecular structure of **AR25** [chemical name: *cis*-bis(2,2′-bipyridyl-4,4′-dicarboxylic acid)(5,6-dimethyl-1,10-phenanthroline)bis(isothiocyanato)ruthenium(II)].

[a] Institute of Chemical Research of Catalonia (ICIQ), Avda. Països Catalans 16, 43007 Tarragona, Spain
Fax: +34-977-920-241
E-mail: epalomares@iciq.es
[b] Institució Catalana per a la Recerca i Estudis Avançats (ICREA), Passeig Lluís Companys 23, 08010 Barcelona, Spain

Results and Discussion

The **AR25** shows a typical UV/Vis spectrum with a metal-to-ligand charge-transfer band (MLCT) centred at λ = 518 nm with a molecular extinction coefficient of 6578 $M^{-1}cm^1$. Figure 1 illustrates the absorption spectra of the complex in solution and adsorbed onto a transparent mesoporous TiO_2 film. As can be seen, the spectra do not show any significant shift, which can be understood as a low or negligible presence of dye molecular aggregates. Moreover, in solution, after excitation at the maximum of the MLCT band, a broad emission band can be observed with a maximum at λ_{em} = 746 nm. The large Stokes shift is due to the nature of the excited state, which – as reported before for other ruthenium(II) complexes[8] – is a triplet energy state. It is worthy to note that the **AR25** emission is strongly quenched when its molecules are anchored to nanocrystalline TiO_2 particles (Figure 2). Hence, we can conclude that the electron-injection process from the excited state into the semiconductor conduction band (CB) is responsible for the immediate disappearance of luminescence upon light excitation. Furthermore, the excited-state emission lifetime for the complex is strongly shortened when anchored to the mesoporous TiO_2 film. The emission lifetime for **AR25** in solution (we used dimethylformamide, DMF, as solvent) gives in our hands a decay that was fitted to two kinetic components, τ_1 = 9.57 ns (18.9%) and τ_2 = 56.67 ns (81.1%) whereas for the **AR25/TiO$_2$** samples τ_1 = 2.23 ns (48.5%) and τ_2 = 12.61 ns (51.5%).

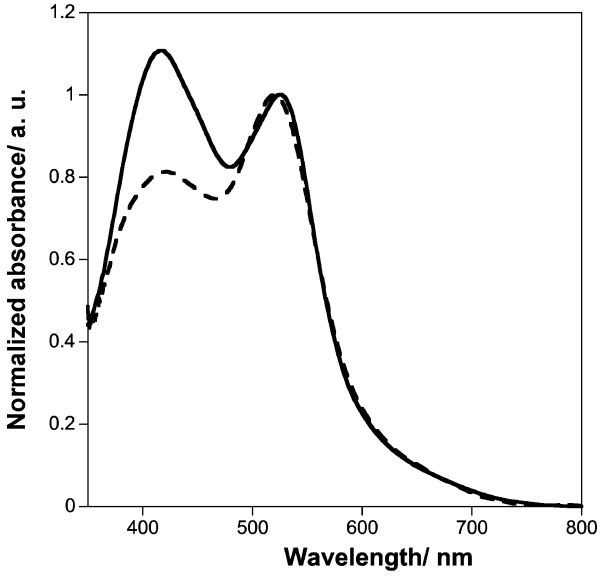

Figure 1. UV/Vis spectra of **AR25** in DMF (1×10^{-4} M, ----) and adsorbed onto a 4 μm thick transparent TiO_2 film (–).

The electrochemical properties of the ruthenium(II) complex **AR25** were also analyzed using cyclic voltammetry (CV) in dry DMF as solvent with 0.1 M tetrabutylammonium hexafluorophosphate as electrolyte. The CV allowed the observation of a quasi-reversible couple at 0.79 V vs. SCE assigned to the $Ru^{II/III}$ redox couple.[9]

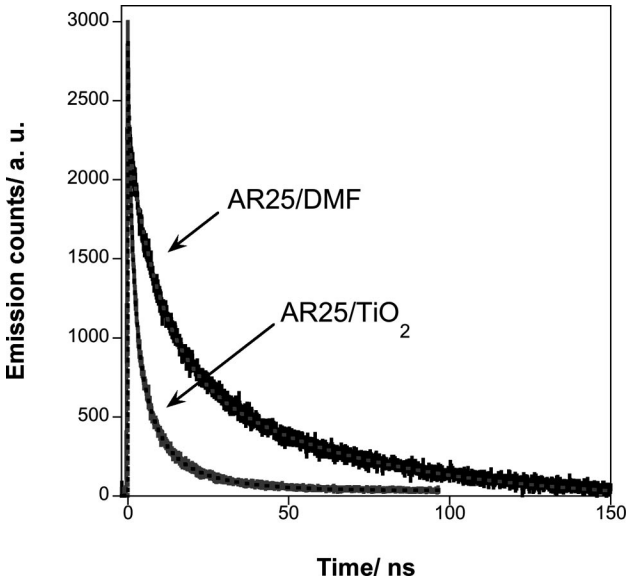

Figure 2. Emission decay kinetics measured using time-correlated single-photon counting under normal conditions for **AR25** in DMF (1×10^{-4} M) and adsorbed onto a 4 μm thick transparent TiO_2 film. Dashed lines correspond to the adjusted fit decay. The excitation wavelength was λ_{ex} = 405 nm, and the emission was monitored at λ_{em} = 745 nm.

Once the electrochemical and the emission properties of the ruthenium complex were measured, we turned to the light-induced charge-transfer kinetics between the sensitizer and the semiconductor nanocrystalline TiO_2 particles. As we have reported before,[10] we have utilized laser-transient absorption spectroscopy (L-TAS) to investigate the electron-recombination dynamics. Figure 3 shows typical decay kinetics for the **AR25/TiO$_2$** samples. We assigned the tran-

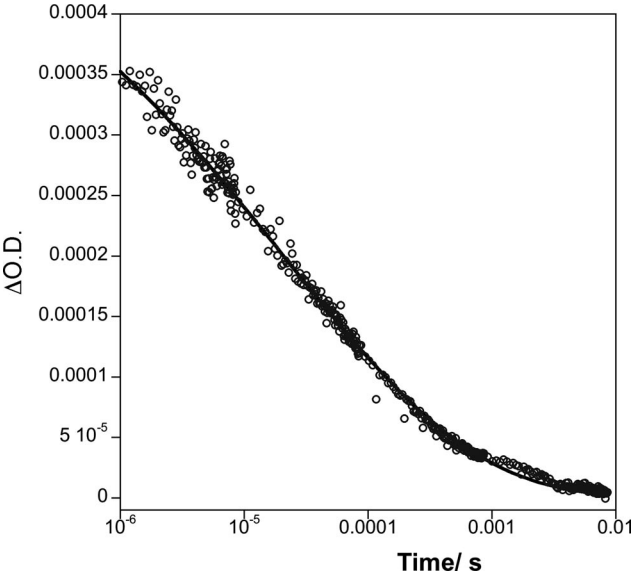

Figure 3. Transient-absorption decay kinetics for a 4 μm thick transparent mesoporous film sensitized with **AR25**. The solid line corresponds to the fitting to a stretched exponential function: $\Delta O.D. = \exp[-(t/\tau)^{\alpha}]$. The excitation wavelength was λ_{ex} = 535 nm and the probe wavelength was λ_{pr} = 800 nm.

sient-decay signal to the recombination of the photo-injected electrons, upon laser excitation, into the semiconductor conduction band and the oxidized dye species. The recorded excited spectra show a broad absorption band with a maximum centred at 800 nm, which has previously been assigned to the cation species of similar ruthenium(II) complexes such as the above-mentioned **N719** molcule.[11] The measurement of the electron-recombination lifetime at the half maximum of the signal is 35 μs.

Finally, we carried out measurements on complete functional devices. We measured the incident photon-to-current conversion efficiency (IPCE) spectra for devices sensitized with **AR25** using as electrolyte a solution containing the redox couple iodine/iodide (see Experimental Section). Figure 4 illustrates the IPCE spectra for an **AR25**/DSSC.

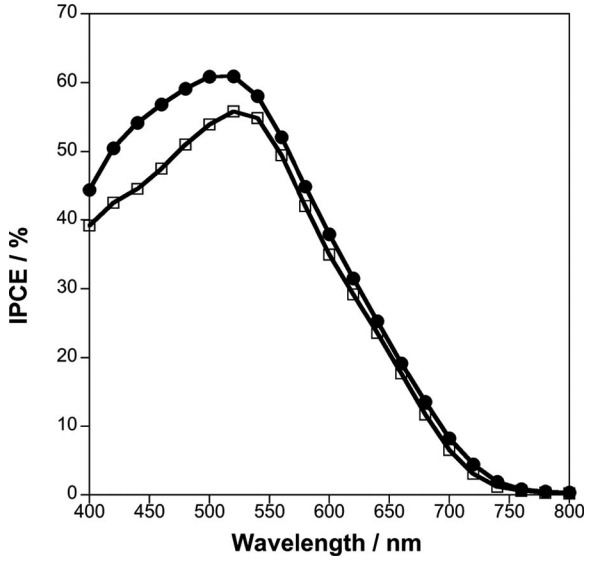

Figure 4. IPCE spectra for DSSC sensitized using **AR25** (full circles) and the homoleptic dye **N719** (empty squares).

In our hands, the IPCE spectrum for **AR25** devices showed higher intensity at the maximum absorption wavelength at λ = 550 nm when irradiated with simulated sunlight. The corresponding photocurrent vs. voltage characteristic curves were also measured to give an overall efficiency of 2.6% under irradiation at 1 sun (100 mW/cm^2) with simulated 1.5 AM G solar spectrum (Figure 5). Under the same conditions, we examined DSSC sensitised with the **N719** dye, and the overall efficiency was 3.6%. The main difference between both devices was in the open-circuit voltage (V_{oc}). While for the former ruthenium(II) complex a V_{oc} = 0.69 V was obtained, for the latter a V_{oc} = 0.78 V was observed. We also noted that the devices made using **AR25** as sensitizer usually showed lower fill factors when compared to devices made using the **N719** complex (38.5% and 47.6%, respectively). We believe that the higher recombination on **AR25** devices limits the photocurrent and the overall performance of the solar cell. Further work focussed on the control of such wasteful reactions is being carried out.

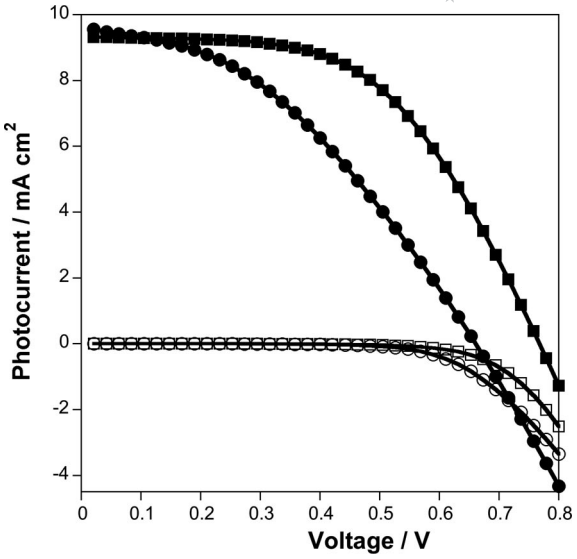

Figure 5. Photocurrent vs. voltage curve (curves I–V) for a 1 cm^2 **AR25** DSSC (circles) and **N719** DSSC (squares). Measurements were performed at 1 sun (full signal) and dark conditions (empty signal).

Conclusions

We presented a new ruthenium(II) heteroleptic complex which shows the appropriated redox electrochemistry to be used as sensitizer in dye-sensitised solar cells. Furthermore, we have characterized the charge-transfer processes occurring at the interface between the **AR25** dye and the nanocrystalline TiO_2 nanoparticles showing that the photo-induced electron injection is particularly efficient despite the low-lying π*-level character of the phenanthroline moiety as coordinating ligand,[12] and the electron recombination processes is at least one order of magnitude slower than the regeneration reactions, which normally occur on the nanosecond time scale; this makes feasible the possibility to optimize the devices and achieve higher light-to-energy efficiencies in the same order of magnitude than the most popular dye, **N719**. The high photocurrent observed using **AR25** makes the dye an interesting candidate for "molecular cocktails" where several dyes with light absorptions in different regions of the solar spectrum are combined to achieve the desired panchromatic sensitization of DSSC.

Experimental Section

Synthesis of AR25: The synthesis of *cis*-bis(2,2′-bipyridyl-4,4′-dicarboxylic acid)(5,6-dimethyl-1,10-phenanthroline)bis(isothiocyanato)ruthenium(II) [Ru(dcbpy)(dmphen)(NCS)$_2$] (**AR25**). The synthesis of **AR25** was carried out according to that reported by Kasuga et al.,[13] but by adding 5,6-dimethyl-1,10-phenanthroline (81.6 mg, 0.4 mmol) instead of 1,10-phenanthroline. Yield: 56.6%. ^{1}H NMR (400 MHz, [D$_7$]DMF): δ = 9.75 (d, J = 5.94 Hz, 1 H), 9.68 (d, J = 5.24 Hz, 1 H), 1.26 (d, J = 1.26 Hz, 1 H), 9.06 (d, J = 1.39 Hz, 1 H), 9.04 (d, J = 8.87 Hz, 1 H), 8.66 (d, J = 8.56 Hz, 1 H), 8.44 (dd, J = 5.80, 1.65 Hz, 1 H), 8.35 (dd, J = 8.56, 5.25 Hz, 1 H), 8.11 (d, J = 5.25 Hz, 1 H), 8.11 (d, J = 5.25 Hz, 1 H), 7.92 (d, J = 5.95 Hz, 1 H), 7.63 (dd, J = 8.45, 5.38 Hz, 1 H), 7.56 (dd,

J = 5.76, 1.34 Hz, 1 H), 2.92 (s, 3 H), 2.81 (s, 3 H) ppm. ESIMS: m/z = 670 [M + H]. FTIR: $\tilde{\nu}$ = 2080 [ν(N=C=S)$_{as}$],1709 [ν(C=O)], 858 [ν(N=C=S)$_{sym}$] cm^{-1}. $C_{28}H_{20}N_6O_4RuS_2$ (670): calcd. C 50.2, H 3.1, N 12.5; found C 53.3, H 5.29, N 11.1.

Optical, Electrochemical and Spectroscopical Measurements: The UV/Vis and fluorescence spectra were recorded using a 1 cm pathlength quartz cell with a Shimadzu UV spectrophotometer 1700 and an Aminco–Bowman series 2 luminescence spectrometer with temperature controller. The electrochemical data was obtained employing a conventional three-electrode cell connected to a CH Instruments 660c potentiostat-galvanostat. For the cyclic voltammetry, we used a platinum working electrode, a calomel reference electrode (SCE) and a platinum wire as auxiliary electrode. The picoseconds to microseconds emission lifetime measurements were carried out with a Lifespec© picosecond fluorescence lifetime spectrometer from Edinburgh Instruments©. As excitation source, the diode laser with 405 nm nominal wavelength was used. The instrument response measurement at the HWHM (half width a high maximum) was below 350 ps. Laser transient-absorption measurements (TAS) were carried out with a home-built system as reported before.[10] ^{1}H NMR spectra, NOESY and COSY experiments were measured with a Bruker 400 MHz spectrometer. A Waters LCT Premier liquid chromatograph coupled to a time-of-flight mass spectrometer (HPLC/MS-TOF) with electrospray ionization (ESI) was used to measure mass spectra.

The FTIR spectra were obtained with an FTIR ThermoNicolet 5700 spectrometer.

Nanoparticle Synthesis and Film Preparation: The nanocrystalline TiO_2 particles were synthesized as reported before.[14] In brief: Titanium isopropoxide (40 mL, 0.13 mol) was added to glacial acetic acid (9.12 g) under argon while stirring. The reaction mixture was cooled in an ice-bath, and 0.1 M nitric acid (240 mL) was added while vigorously stirring. The mixture was heated in an oil bath at 80 °C during 8 h. and, after cooling, was filtered through a 0.45 μm syringe filter. The resulting product was diluted to 5 wt.-% of TiO_2 by adding water and then autoclaved at 220 °C for 12 h. The aqueous phase was removed by centrifugation, and the solid nanoparticles were isolated and rinsed twice with ethanol. An ultrasonic horn was used to break the aggregates, and the solvent was removed under vacuum. The solid nanoparticles were diluted to 15 wt.-% in TiO_2, using ethyl cellulose and terpineol, and the paste was homogenized by using a ball mill.

Device Preparation and Characterization: DSSCs were made using 4 μm thin films consisting of 20 nm TiO_2 nanoparticles deposited onto a conducting glass substrate (Hafford Glass Inc., 15 Ω/cm^2 resistance) by using the well-known doctor-blade technique. The active area was 0.152 cm^2. The as-prepared electrodes were gradually heated under airflow at 325 °C for 5 min, 375 °C for 5 min, 450 °C for 15 min, and 500 °C for 15 min. Then, they were submerged into 40×10^{-3} M $TiCl_4$ aqueous solution at 70 °C for 15 min, washed with ethanol, heated again at 500 °C for 30 min, and cooled to 50 °C before soaking the films in a 5×10^{-4} M **AR25** solution in acetonitrile/*tert*-butyl alcohol (1:1) overnight. The counter electrodes were prepared by spreading a solution of H_6PtCl in ethanol onto a conducting glass substrate with a small hole to allow the introduction of the liquid electrolyte, under vacuum. The liquid electrolyte was prepared by using 0.6 M DMPII (1-propyl-2,3-dimethylimidazolium iodide), 0.05 M I_{22}, and 0.1 M LiI in acetonitrile/valeronitrile (85:15). The photovoltaic measurements were carried out with a 150 W xenon lamp from Oriel Instruments with the appropriated set of filters for the correct simulation of the 1.5 AM G solar spectrum. The incident light power was calibrated by using a silicon photodiode previously calibrated at 1000 W/m^2 at 1.5 AM G.

Acknowledgments

E. P. would like to thank the Spanish Ministerio de Educación y Ciencia (MEC) for the funding through the CONSOLIDER-HOPE-CSD-0007-2007 and the CTQ2007-60746/BQU project. E. M. F. also thanks the MEC for her Juan de la Cierva Fellowship.

[1] N. Robertson, *Angew. Chem. Int. Ed.* **2006**, *45*, 2338–2345.
[2] M. Gratzel, *Prog. Photovolt.* **2006**, *14*, 429–442.
[3] J. R. Durrant, S. Haque, E. Palomares, *Coord. Chem. Rev.* **2004**, *248*, 1247–1257.
[4] M. K. Nazeeruddin, C. Klein, P. Liska, M. Gratzel, *Coord. Chem. Rev.* **2005**, *249*, 1460–1467.
[5] C. Klein, M. K. Nazeeruddin, D. D. Censo, P. Liska, M. Gratzel, *Inorg. Chem.* **2004**, *43*, 4216–4226.
[6] D. Kuang, C. Klein, S. Ito, J. E. Moser, R. Humphry-Baker, N. Evans, F. Duriaux, C. Grätzel, S. M. Zakeeruddin, M. Grätzel, *Adv. Mater.* **2007**, *19*, 1133–1137.
[7] C. S. Karthikeyan, H. Wietasch, M. Thelakkat, *Adv. Mater.* **2007**, *19*, 1091–1095.
[8] J. R. Lakowicz in *Principles of Fluorescence Spectroscopy*, 2nd ed., Kluwer Academic/Plenum Publishers, New York, **1999**.
[9] M. Yanagida, L. P. Singh, K. Sayama, K. Hara, R. Katoh, A. Islam, H. Sugihara, H. Arakawa, M. K. Nazeeruddin, M. Gratzel, *J. Chem. Soc., Dalton Trans.* **2000**, 2817–2822.
[10] S. Tatay, S. Haque, B. C. O'Regan, J. R. Durrant, W. Verhees, J. Kroon, A. Vidal-Ferran, P. Gaviña, *J. Mater. Chem.* **2007**, *17*, 3037–3044.
[11] S. Haque, E. Palomares, B. Cho, A. Green, N. Hirata, D. Klug, J. R. Durrant, *J. Am. Chem. Soc.* **2005**, *127*, 3456–3462.
[12] D. J. Stufkens, A. Vlcek Jr, *Coord. Chem. Rev.* **1998**, *177*, 127–179.
[13] N. Onozawa-Komatsuzaki, O. Kitao, M. Yanagida, Y. Himeda, H. Sugihara, K. Kasuga, *New J. Chem.* **2006**, *30*, 689–697.
[14] S. Hore, E. Palomares, H. Smit, N. J. Bakker, P. Comte, P. Liska, K. R. Thampi, J. M. Kroon, A. Hinsch, J. R. Durrant, *J. Mat. Chem.* **2005**, *15*, 412–418.

Received: January 16, 2008
Published Online: March 26, 2008

